Engineering Structures 191 (2019) 358–369

Contents lists available at ScienceDirect

Engineering Structures

journal homepage: www.elsevier.com/locate/engstruct

Aggregate effect on concrete cone capacity

Krešimir Ninčević[a], Ioannis Boumakis[a], Marco Marcon[a], Roman Wan-Wendner[a,b,*]

[a] Christian Doppler Laboratory, University of Natural Resources and Life Sciences Vienna, Peter-Jordanstr. 82, 1190 Vienna, Austria
[b] Magnel Laboratory for Concrete Research, Ghent University, Tech Lane Ghent Science Park – Campus A, Technologiepark-Zwijnaarde 60, 9052 Ghent, Belgium

ARTICLE INFO

Keywords:
Concrete
Aggregate
Mechanical anchors
Aggregate effect
Concrete cone capacity
Photogrammetric analysis

ABSTRACT

Recently, a large experimental campaign was completed that attempted to establish a link between petrography of the coarse aggregate, the concrete material properties and the system response in terms of concrete cone capacity. The investigation focused on three normal strength concretes having different coarse aggregate types (quartz, limestone, basalt) but otherwise similar mix design. All specimens of each concrete were cast from the same batch, carefully cured following three sets of curing protocols, and systematically characterized. The investigation comprised aggregate and concrete characterization, and structural tests performed at two ages on cast-in headed stud anchors under tensile loading. The aggregate characterization included the determination of Los Angeles coefficient, hardness and Young's modulus. In order to characterize the concretes, standard compression and indirect tension tests, were performed together with fracture tests. The experimentally obtained material and structural data finally served for the evaluation of current predictive models in terms of concrete compressive strength or concrete fracture properties as well as a correlation study. Aided by photogrammetric analysis, the concrete cone shape was determined for each individual test and analyzed to uncover possible dependencies on the coarse aggregate type.

1. Introduction

Concrete is the fundamental structural material in the civil engineering industry. Over the last years it became one of the most used building materials. Fresh concrete can be cast easily into almost every shape. It is characterized by good mechanical properties (e.g. compressive strength) that are improving steadily with time due to ongoing hydration. Hence, it has almost unlimited applications in the modern construction industry.

Fastening elements are an essential component of modern construction as they allow the connection of load bearing structural members and the installation of necessary equipment. The increasing age of our built infrastructure in combination with the rising awareness towards the environmental impact of the construction industry have further promoted the application of fastenings e.g. for strengthening and rehabilitation. Other trends such as fast modular construction also profit from recent advances in fastening technology. Depending on the specific properties of a chosen fastening system and the loading conditions a number of different failure mechanisms can occur, independently or in combination. One of the most critical failure mechanisms is described by the concrete cone capacity, i.e. the load necessary to rip out a fastening element by exceeding the load bearing capacity of the substrate material resulting in a cone like concrete break-out body attached to the fastening element.

It is well know that concrete is a cementitious composite material – a mixture of cement, aggregate and water. Every component of the concrete mix design affects the properties of concrete. The aggregates take around 70–80% of the concrete volume and almost 90% of the total concrete weight. Consequently, they play also an important role in defining concrete thermal and mechanical properties. At early age, aggregates determine the workability, where the aggregate shape, surface roughness and type influence the interaction and bond between paste and aggregates [1]. The aggregate surface texture can be either rough or smooth, depending on the mineralogical type and the origin of the aggregates. Rougher surface results in a higher adherence and bond strength between the cement paste and the aggregates [2], while a smooth surface leads to better concrete workability during casting.

In the past, many researchers investigated the aggregate effect on concrete properties, mostly on the concrete compressive strength. Delmar et al. [3] confirmed that at the same water to cement ratios, smaller sizes of aggregate lead to higher concrete strengths. On the other side, Vilane et al. [4] reported an increase of compressive strength with increasing aggregate size in a range of 9.5–19 mm. Özturan and Çeçen [5] studied the effects of coarse aggregate type on concrete

* Corresponding author at: Christian Doppler Laboratory, University of Natural Resources and Life Sciences Vienna, Peter-Jordanstr. 82, 1190 Vienna, Austria.
E-mail addresses: kresimir.nincevic@boku.ac.at (K. Ninčević), roman.wanwendner@ugent.be (R. Wan-Wendner).

https://doi.org/10.1016/j.engstruct.2019.04.028
Received 29 August 2018; Received in revised form 15 March 2019; Accepted 9 April 2019
Available online 03 May 2019
0141-0296/

mechanical properties. They reported that normal strength concretes with gravel and basalt aggregate result in similar compressive strength, and limestone concrete resulted in a higher strength. These conclusions depend not only on the used aggregate type but also on its exact mineralogical structure, and on other concrete mix composition parameters (e.g. water content, water to cement ratio, amount of fine and coarse aggregates and their granulometric distribution). They also reported that the strength of the interface between aggregate and cement paste governs the behaviour of concrete in unconfined compression tests. This is a valid statement, especially in case of normal strength concretes, where the mortar and bond strength are much lower than aggregate strength. An aggregate shape study performed by Guinea et al. [6] showed that concretes with broken aggregates are characterized by higher fracture properties.

In current concrete design codes [7,8] concrete is typically characterized by compressive strength only, a convenient choice. All the other material properties are expressed in terms of compressive strength by empirical equations that rarely account for the mix design or type of coarse aggregate. However, since concrete is used worldwide, the possible sources of aggregates and, thus, their properties vary widely. Consequently, different mix designs are generally required in order to obtain the same compressive strength class, potentially affecting other material properties in an unforeseeable way.

Fastening related design and approval guidelines [9–13] follow the same practically convenient approach and formulate concrete related failure mechanisms in terms of concrete compressive strength. Even though the concrete cone capacity is determined by fracture-mechanics (and related material properties) the established design equation is formulated in terms of compressive strength.

This contribution presents the experimental investigation of a possible aggregate effect on the concrete cone capacity beyond the direct affect that is captured by the current predictive equations in terms of concrete material properties. The standard approach using compressive strength [14] is compared to a fracture mechanics alternative [15]. After a thorough review of the state of the art, the experimental campaign is presented comprising three concrete batches with different aggregate type (basalt, limestone, and quartz). Structural tests were performed on cast-in headed stud anchors under tensile loading at 28 days and 70 days. Along with the structural tests, each concrete was fully characterized to determine all standard concrete properties (modulus, compressive and tensile strength, and fracture energy) at the same ages when the structural tests were performed. Additionally, the aggregates have been characterized. Available measurements include the Los Angeles coefficient (L.A.), hardness and Young's modulus, the latter two obtained by grid indentation on representative coarse aggregate pieces. Finally, all available material and structural test data, including the photogrammetrically obtained cone shapes, are analyzed for relevant dependencies.

2. State of the art

In this chapter a short overview of the currently established predictive models for the concrete cone capacity is presented. The second part of this chapter is focused on aggregate effect studies performed in the past by other research groups on concretes, and anchors.

Current design codes and approvals [9–13] mostly specify minimum requirements for the aggregates, where it is suggested to use aggregates of medium hardness. However, they provide no guidance about the aggregate type in a petrographical sense. Typically, the cement type is defined, together with restrictions for the cement content and water to cement ratio. Finally, two standardized concrete strength classes were defined to be used for anchor tests and approvals. They are deemed to be representative for the situation on common construction sites.

In general, for mechanical anchors under tensile loading different failure mechanism can occur, ranging from steel failure, pull-out and pull-through failure, to concrete related failure modes such as concrete cone breakout and concrete splitting [16]. The focus of this investigation lies on the concrete cone breakout failure mechanism. Consequently, the experimental program and the fastenings were designed accordingly, forcing concrete cone failure. Other failure mechanisms in tension were not investigated in this study.

After years of comprehensive and thorough anchor related research [17–25], two main predictive models were proposed. Fuchs et al. [14] first proposed a relatively simple and user-friendly empirical model to predict the concrete cone capacity. This predictive model is well know as concrete cone capacity design (CCD) method. The mean concrete cone capacity N_{CCD} of a single anchor loaded in tension is given by Eq. (1).

$$N_{CCD} = k \cdot h_{ef}^{1.5} \cdot \sqrt{f_c} \tag{1}$$

According to the CCD predictive model (Eq. (1)), the pull-out load capacity N_{CCD} [N] is a function of a product-dependent calibration factor k with dimensional units [$N^{0.5}/mm^{0.5}$], the concrete cube compressive strength f_c [MPa] (cube with 200 mm sides), and the anchor embedment depth h_{ef} [mm]. For headed studs, current design codes recommend a factor $k = 15.5$ even though a head-size dependence is known to exist [26–28]. Herein it has to be noted that all presented analyses are based on 150 mm cube compressive strength values that have been converted to 200 mm cube strengths using the code recommended conversion factor of 0.95 ($f_{c,200mm} = 0.95 \cdot f_{c,150mm}$) [29]. Additionally, the analysis was also performed on cylinder compressive strengths, yielding of course different k values but the same overall trend, i.e. insignificant aggregate effect after normalisation.

Knowing the fracture mechanical nature of the problem, Eligehausen and Savade [15] also proposed a more mechanically rigorous model given by Eq. (2). Herein, the pull-out load capacity N_{EG_F} [N] is a function of a factor n, the anchor embedment depth h_{ef} [mm], concrete elastic modulus E, and concrete total fracture energy G_F. The critical value of $n = 2.1$ relates the load capacity of the anchor (peak load) to the length of the already propagated crack at the loss of stability compared to it's extrapolated total crack length up to the concrete surface. It has to be noted that the tensile strength of concrete is already exceeded well before the peak load is reached and a crack started to propagate. Thus, what determines the load capacity is an energy balance between the elastically stored energy in the system and the work required to propagate the crack. However, this fracture mechanical model is not widely used. The main reason can be found in the difficulties to experimentally determine the concrete fracture energy, further amplified by the typically high scatter in such experiments.

$$N_{EG_F} = n \cdot h_{ef}^{1.5} \cdot \sqrt{E \cdot G_F} \tag{2}$$

In both cases the design equations used to predict the concrete cone capacity are only taking into account the concrete material properties, regardless of the used mix design, or aggregate type. Considering the complex heterogeneous nature of the composite material concrete, it is clear that its properties depend not only on the individual components but also on their interaction.

Many researchers performed studies on headed stud anchors, focusing on different problems such as e.g. concrete and its effect on the anchor capacity. Primavera et al. [30] studied the anchor capacity for normal and high strength concretes. Since concrete ages and changes its properties over time, Winters et al. [31] studied the concrete breakout capacity in early-age concrete. A study performed on anchors installed in cracked and uncracked concrete was reported by Eligehausen et al. [32]. Over time the cast-in headed stud anchor became the paratype of fastening element for the investigation of the concrete cone capacity even though also in this case features of the anchor influence the peak load. Recently, Nilforoush et al. reported the results of an investigation into the influence of the concrete slab thickness and the effect of the anchor head size on the load capacity [27,28]. Apart from experimental investigations, also numerical studies have been used successfully in

fastening research. Reliable numerical models allow the cost-efficient extension of the experimentally investigated parameter range to untested configurations. Furthermore, it is possible to decouple phenomena, perform sensitivity studies and gain insights into more complex situations that cannot be directly measured. However, it is important that the models are properly calibrated and validated. Only then, extrapolations can be trusted. Ozbolt and co-workers [33,34] studied numerically the embedment depth effect on the performance of anchor bolts. Hordijk et al. [35] attempted to study the aggregate effect on headed stud anchors but was not able to complete the study due to steel failure. Rodriguez et al. [36] performed dynamic tests of anchors under tensile loading. The results indicated that the type of aggregate has no significant effect on the normalized tensile capacity, covering concretes with soft limestone aggregate to medium-hard river gravel aggregates.

Despite various studies documented in the literature there is still a lack of comprehensive experimental investigations that include the characterization of coarse aggregates, a full (fracture mechanical) concrete characterization, and anchor pull-out data. The authors are not aware of any available systematic analysis that aimed at identifying the relationship between aggregate properties, concrete properties, and concrete cone capacity. Therefore, in this study such pairwise dependencies are investigated including a potentially remaining effect between concrete cone capacity and aggregate properties, that is after removing the dependency on the standard concrete material properties based on the two established prediction models introduced earlier.

3. Experimental investigation

3.1. Overview

In 2016–2017 a comprehensive experimental campaign was performed comprising aggregate and concrete characterization, and structural tests. Structural tests were performed in tension on cast-in headed stud anchors for one embedment depth. Both concrete material and structural test were performed twice, once at 28 and once at 70 days. In total 90 cubes, 70 cylinder, 24 prisms and 12 slabs were cast.

Selected representative coarse aggregate pieces served for the characterization of the aggregates by standard Los Angeles tests and grid-indentation. On top of load displacement data also the shape of the break-out cones was documented by means of photogrammetry. Finally, all available data was analyzed systematically in order to unearth dependencies and new insights.

3.2. Mix design

For the purpose of this experimental investigation, in total three normal strength concretes were investigated. All the concretes used the same CEM II 42.5 N cement and aimed at the strength class C25/30. The sieve curve of each concrete was selected according to ETAG guidelines [29].

The main difference between the three concretes can be found in the petrography and the granulometric distribution of the used coarse aggregate. It is important to note that the basalt aggregates could not be obtained with a maximum aggregate size of 16 mm, and therefore a maximum aggregate size of 22 mm was used for concrete batch E3. As discussed earlier the petrography and size are just a few of the many aggregate related influence factors on concrete material properties. All the other ones were not controlled.

The other mix design parameters, such as water to cement (w/c) and aggregate to cement (a/c) ratio, remained almost constant. The exact values and differences of all three mix-designs are listed in Table 1. It has to be noted that the mix designs cover some of the most typical aggregates found in Europe while balancing practical considerations such as prolonged workability during casting and availability of ready-mix concrete.

Table 1
Exact concrete mix design for all batches.

Batch	Unit	E1	E2	E3
Water content	[kg/m^3]	173.2	163.6	167.8
Cement content	[kg/m^3]	274.9	274.8	289.5
Aggregate shape	[–]	round	round	broken
Aggregate type	[–]	quartz	limestone	basalt
Fine aggregates: 0–4 mm	[kg/m^3]	838.4	1185.3	750.2
Coarse aggregates: 4-D_{max}	[kg/m^3]	1066.1	811.7	1330.1
D_{max} = max aggregate size	[mm]	16	16	22
Total amount of aggregates	[kg/m^3]	1904.5	1997.0	2080.3
Water to cement ratio	[–]	0.63	0.60	0.58
Aggregate to cement ratio	[–]	6.93	7.27	7.19

3.3. Curing protocols

Specimens and slabs alike were cured inside the moulds for the first 24 h. After that, they were removed from the moulds preventing any exposure to adverse conditions and impacts. The specimens for the material characterization were stored according to three different curing protocols until the day of testing (at an age of 28 or 70 days, respectively). The three curing protocols were selected in an attempt to (i) satisfy the material testing standards, (ii) satisfy anchor approval guidelines, and (iii) test specimens that may better represent the conditions inside an aging and drying concrete slab.

Most material testing standards [37,38] require specimens to be cured either in lime-saturated water or in high-humidity moist curing rooms. Both conditions avoid drying and ensure sufficient water availability such that the desired hydration state and material properties can be reached. Consequently, also empirical equations linking the concrete material properties E_c, f_c, f_t, and G_F apply to moist-cured specimens. In this study one set of specimens was cured in lime-saturated water at ambient laboratory temperature of around 23 °C. These specimens are referred to as “moist-in”. However, this curing protocol is not in agreement with the anchor related codes [29], which require the specimens for the material characterization to be stored next to the concrete members for the structural (anchor) tests. Consequently, a second set of specimens was stored with the slabs outside, in front of the laboratory, undergoing the same environmental temperature and humidity histories. This set of specimens was named “dry-cured”. Additionally, a third set of specimens, named “moist-out”, was stored in lime-saturated water in front of the laboratory and next to the “dry-cured” specimens and slabs , thus following the same temperature history without impact on the water balance.

3.4. Aggregate characterization tests

Mechanical properties of each used aggregate type were obtained by nano-indentation on representative coarse aggregate pieces and standard abrasion tests. Nano-indentation is a well established and effective test method to determine elastic material properties on the microscopic scale [39–41]. The advantage of this method over some other conventional methods is the possibility to perform tests on extremely small samples and thin layers of material. In nano-indentation tests a small tip called indenter is pressed into the previously prepared smooth sample surface. The tip is held in place for a defined duration and sequentially released generating a load-displacement curve. The specific tests were performed using a Berkovich tip nano-indenter. It is a type of the indenter with the geometry of a three-sided pyramid, and is usually used to identify the hardness of materials. After the initial load of F_{ini} = 150 mN was applied, the load was held for t = 30 s before the unloading started. Considering the sensitivity of the nano-indenter, this

Table 2
Experimentally obtained aggregate properties.

Aggregate type	L. A. coefficient [–]	Modulus [GPa]	Hardness [GPa]
Quartz	26.0	11.4	0.5
Limestone	22.6	37.5	1.4
Basalt	15.0	45.6	2.3

loading regime minimizes thermal effects and drifts of vibrations during measurement.

Standard Los Angeles (L.A.) abrasion tests were performed to identify aggregate toughness and abrasion [42]. This type of test is a common test method to evaluate a coarse aggregates abrasive resistance by placing aggregates inside a rotating steel drum. The steel drum contains a certain number of steel spheres. As the steel drum rotates the repeated collision with the spheres and aggregate pieces results in severe abrasion. The experimentally obtained mechanical aggregate properties are listed in Table 2.

The results shown in Table 2 indicate that the quartz aggregate is the softest aggregate among the three different aggregate types, while the basalt aggregate is the strongest and hardest aggregate. Additionally, Fig. 1 shows representative photos obtained during nano-indentation tests in which the large differences in coarse aggregate composition and micro-structure can be observed. Typically, all aggregates with an L.A. coefficient below 30 can be considered strong, and can be used in coating or road industry. The obtained L.A. abrasion values are in good agreement with the available literature data [2]. Comparing the L.A. coefficients with the modulus or hardness of the aggregate, a clear trend can be noticed confirming that lower L.A. coefficients correspond to tougher aggregates and a larger resistance against abrasion.

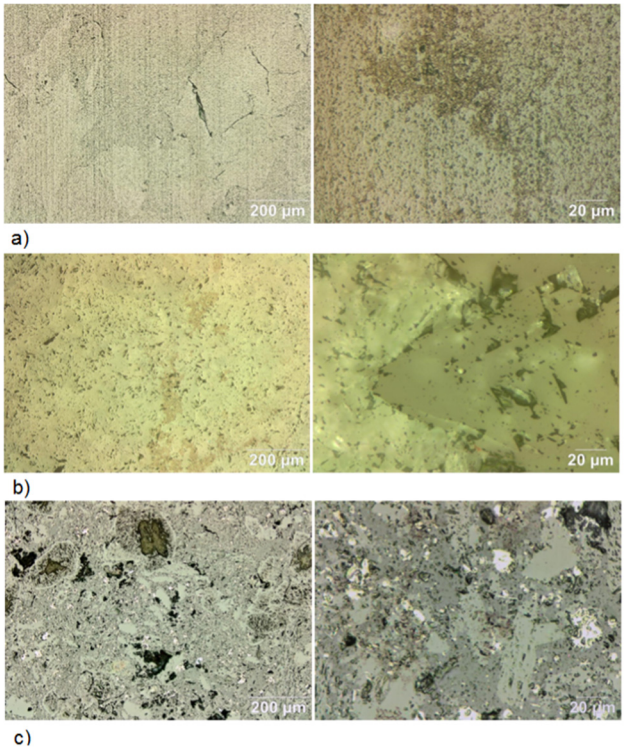

Fig. 1. Representative photos obtained during nano-indentation tests with a light microscope for (a) quartz, (b) limestone, and (c) basalt aggregate type.

3.5. Concrete characterization tests

The concrete characterization tests were performed in parallel to the structural pull-out tests, i.e. on the same day when the anchor tests were performed. Standard concrete specimens (cubes, cylinders and prisms) were tested to identify the concrete properties for each of the previously introduced curing protocols. Typically, these tests were carried out using five specimens of the same type, curing protocol, and age.

In order to identify concrete compressive strength ($f_{c,cu}$ and $f_{c,cyl}$), cubes with a side length of 150 mm, and cylinders with 150 mm diameter and 300 mm height were tested according to [43]. The cylinders tests were instrumented with three LVDT's (HBM Displacement Transducers WI/5 mm-T) spaced equiangularly around the perimeter with a base length of 100 mm. These on-specimen measurements allow the determination of load eccentricities and, averaged, provide an accurately estimate of the loading modulus (E). Both cube and cylinder compression tests were performed with a rate of loading of 0.008 mm/s.

The indirect tensile strength properties ($f_{t,spl}$) were obtained performing Brazilian splitting tests [44] on cylindrical specimens with a diameter of 150 mm and a height of 70 mm with the constant loading rate of 0.02 mm/s. All compression and Brazilian splitting tests were performed using a 5 MN Walter & Bai load frame.

Three point bending tests were performed on notched prisms with dimensions of 100 × 100 × 400 mm, a relative notch depth of 30% and a span of 300 mm in order to determine concrete fracture properties. These tests were performed using the servo hydraulic testing machine Walter & Bai LFV-63 kN. In order to ensure stable tests and especially post-peak response, the tests were controlled by crack mouth opening displacement (CMOD). A constant loading rate equal to 0.0001 mm/s was applied using an extensometer of type Epsilon 3542-050M-025-HT2. The total fracture energy (G_F) presented in this study is determined by the work of fracture method, i.e. by integrating the area under the load load-point displacement diagram until the specimen is fully softened and relating the total work performed to the fracture surface created (ligament area). The inverse analysis of the cohesive law based on load-opening diagrams are reported for all three concretes and both ages in [45].

In general, fracture energy is defined as the energy needed to create a unit fracture surface, and it is one of the most important concrete properties, especially in analyses where fracture and damage propagation matter. In case of headed stud anchors under tensile loading, crack propagation starts at the anchor head when the crack formation energy and the tensile strength limits are reached [16,46].

The mean results of the concrete characterization tests for all concretes are shown in Table 3 together with the corresponding coefficients of variation (CoV). The listed values are representative of "moist-in" specimens (as required by material standards) and were obtained by five tests each. Additionally, the corresponding compressive strength values for cubes ($f_{c,cu}^{dry}$) and cylinders ($f_{c,cyl}^{dry}$) obtained according to the anchor approval guidelines are presented in Table 4, together with the structural results.

Comparing the obtained aggregate properties from Table 2, and concrete compressive strength results from Table 3, it can be concluded

Table 3
Experimentally obtained material properties for moist-in cured specimens.

Concrete	$f_{c,cu}$ [MPa]	$f_{c,cyl}$ [MPa]	$f_{t,spl}$ [MPa]	E [GPa]	G_F [N/m]
E1-28 d	34.3 ± 6.2%	32.3 ± 7.7%	3.0 ± 20.8%	30.6 ± 8.1%	95.3 ± 15.4%
E2-28 d	40.3 ± 4.2%	33.9 ± 9.7%	4.1 ± 3.3%	31.4 ± 11.2%	73.8 ± 8.3%
E3-28 d	42.1 ± 4.9%	36.3 ± 6.7%	3.4 ± 2.0%	31.8 ± 4.0%	108.2 ± 13.2%
E1-70 d	38.7 ± 7.6%	36.5 ± 2.9%	3.4 ± 8.6%	31.2 ± 7.5%	84.5 ± 10.7%
E2-70 d	45.6 ± 4.3%	44.8 ± 6.4%	4.4 ± 4.2%	42.2 ± 6.4%	79.9 ± 12.2%
E3-70 d	46.7 ± 9.6%	39.4 ± 6.2%	3.5 ± 9.1%	34.4 ± 5.6%	95.8 ± 14.8%

Table 4
Experimentally obtained tensile load capacities and concrete cube and cylinder compressive strength for "dry" cured specimens.

Concrete	$f_{c,cu}^{dry}$ [MPa]	$f_{c,cyl}^{dry}$ [MPa]	N_{exp} [kN]
E1-28 d	29.1 ± 5.0%	28.4 ± 2.2%	111.2 ± 8.3%
E2-28 d	35.3 ± 3.4%	35.6 ± 2.5%	136.6 ± 9.6%
E3-28 d	35.0 ± 6.3%	33.0 ± 5.8%	124.4 ± 1.2%
E1-70 d	30.6 ± 5.5%	35.9 ± 5.8%	143.4 ± 4.9%
E2-70 d	40.0 ± 6.7%	40.2 ± 5.6%	183.4 ± 7.0%
E3-70 d	39.7 ± 8.0%	35.6 ± 6.7%	173.9 ± 5.6%

that the compressive strength of concrete increases as the hardness of the aggregate increases. The dry-cured specimens exhibit consistently lower compressive strengths compared to the "moist-in" values.

3.6. Structural tests

Structural pull-out tests were performed using a servo hydraulic three axial testing machine with a maximum load equal to 630 kN (both for tension and compression). These test were performed on concrete slabs with dimensions 2.5 × 1.0 × 0.3 m, using cast-in headed studs made of M16 hex-bolt screws with steel grade 12.9. In order to ensure a stiff head with a size comparable to standard headed studs (Nelson type) that can be found on the market, a stiff 6 mm thick washer with a diameter of 32 mm (two times anchor rod diameter) was welded to the smooth anchor rod, as it is shown in Fig. 2(a).

Pull-out tests were performed at 28 and 70 days, for an embedment depth of h_{ef} = 100 mm. Four pull-out tests were performed for each concrete and concrete age. The concrete slab dimensions were optimized to ensure (i) no cross-influence of adjacent anchors by overlapping cones, (ii) sufficient edge distance, and (iii) sufficient slab thickness of three times embedment depth ($h = 3 \times h_{ef}$) to avoid splitting or noticeable influence of bending. All pull-out tests were performed under quasi- static tensile loading and were supported with a stiff circular ring with inner diameter equal to four times the anchor embedment depth ($d = 4 \times h_{ef}$). The ring with the thickness equal to 30 mm had an outer diameter of 600 mm. This configuration is know as "unconfined pull-out test" [29] in the fastening community, and results typically in a cone shaped concrete breakout body (Fig. 2b). This condition excludes any bias of the boundary condition on the peak-load but may still influence the post-peak response and shape of the concrete cone. The tensile load was applied with a spherical coupling controlled by one of two linear variable differential transformers (LVDT) installed close to the concrete surface in order to ensure a constant displacement rate of 0.008 mm/s and stable post-peak response. The HBM LVDTs (I-WA/20 mm-T) had a nominal measuring range of 20 mm, and typical 0.1–0.2% non-linearity. Finally, the anchor displacement was calculated as a mean value out of both LVDTs. More details on the experimental set-up and sketches are provided in a previous study by Ninčević et al. [47].

Experimentally obtained concrete cone capacities for all concretes and ages are listed in Table 4. Each peak value in the table represents the mean value out of four tests and contains information about the coefficient of variation (CoV). It can be noticed that the concrete with quartz aggregates (E1) has a lower mean concrete cone capacity compared to the other two concretes (E2, E3) tested at 28 days. The obtained trend is also confirmed at 70 days, where the concrete with limestone aggregates (E2) showed the highest concrete cone capacity. The comparison with the concrete properties presented in Table 3 reveals a similar relative structure for both ages, i.e. the results for E2 and E3 being similar and substantially lower for E1.

4. Results and discussion

In the following chapter, the experimental data obtained on the material and structural scales for all three concretes will be analyzed in different ways in an attempt to identify dependencies and confirm/reject the hypothesis of an aggregate effect on the concrete cone capacity. Naturally, there is an effect of the used aggregate type on concrete properties and, in turn, on the concrete cone capacity. What is of interest here is the question whether there is an additional effect that is not implicitly captured by current predictive models that are formulated in terms of compressive strength or the product of fracture energy and Young's modulus.

4.1. Comparison of normalized concrete capacities

Obviously, changes in mix design and the choice of the coarse aggregate will result in changing concrete properties. Consequently, it is important to remove the known and expected functional dependencies in order to isolate any remaining additional effect that cannot be fully explained by the currently established prediction models and their (material related) input parameters. The most basic approach to remove dependencies for multiplicative models is normalization as ratio between experimentally obtained anchor load capacity N_{exp} and model predictions N_{CCD} according to Eq. (1) or N_{EG_F} based on Eq. (2).

$$\frac{N_{exp}}{N_{CCD}} = \frac{N_{exp}}{k \cdot h_{ef}^{1.5} \cdot \sqrt{f_c}} \tag{3}$$

$$\frac{N_{exp}}{N_{EG_F}} = \frac{N_{exp}}{n \cdot h_{ef}^{1.5} \cdot \sqrt{E \cdot G_F}} \tag{4}$$

The existence of additional dependencies can be detected based on the amount of variability in the normalized results which can be measured e.g. as coefficient of variation. This variability encompasses measurement errors, material uncertainty, and model errors. Thus, only values exceeding typical levels of experimental scatter indicate the

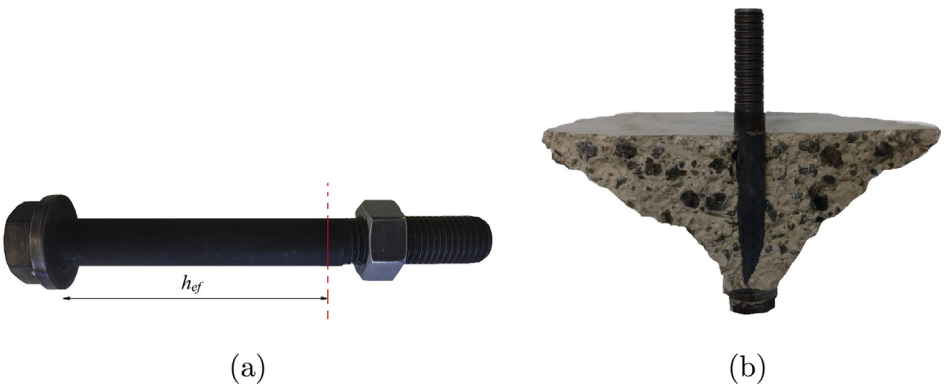

Fig. 2. (a) Headed stud anchor type, and (b) typical concrete cone breakout.

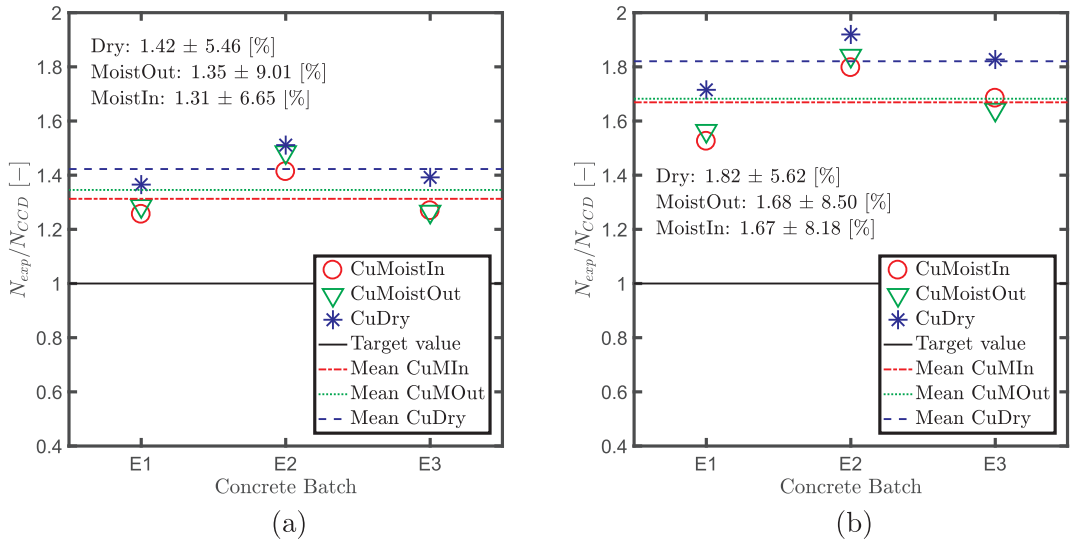

Fig. 3. Normalized concrete cone capacity using the compressive strength based prediction model according to Eq. (3) for (a) 28 days, and (b) 70 days results.

presence of additional effects. Another objective could be the mean value after normalization close to one. However, this second approach is more a test of a good calibration (correct k value) than of the equations' ability to capture the functional dependence between input parameter and response quantity. A sensitivity/correlation study may then reveal additional dependencies and potentially also their functional form if the dataset is sufficiently large.

Normalization using the current predictive equations should ideally result in 1.0 and in a low scatter around the target value, which would mean that the current predictive models are able to accurately predict the anchor load capacity and capture all relevant phenomena. In that case, the concrete compressive strength, or product of modulus and fracture energy, would be sufficient to characterize concrete in a mechanical sense, regardless of the aggregate type.

Fig. 3 shows the tensile capacities normalized by compressive strength using Eq. (3), both for (a) 28 days, and (b) 70 days, respectively. The normalization is performed for all three curing protocols investigated in this study. Note that according to design guides the "moist-in" strength should be used while the anchor approval documents require the use of "dry" cured specimens for the material characterization, i.e. specimens stored with the slabs. For both ages the normalized values are higher than 1.0, indicating that the predictive model, Eq. (1), is conservative for this specific anchor type regardless of the tested concrete curing conditions. Indeed, the use of concrete strength obtained for "dry" curing conditions (as required by anchor approval documents) leads to more conservative concrete cone breakout capacities than the "moist-in" and "moist-out" curing conditions. Naturally, the calibration coefficients could have been re-calibrated to account for this offset. Differences between the normalized values (shown in the Figure as CoV) exist for both ages and all three curing protocols and follow the same trend in each case. This indicates the presence of additional effects that are not represented fully by the model in terms of concrete compressive strength only. However, the analysis also reveals that this effect is minor. With less than 6% difference for the dry-cured case the normalized data lies within the range of typical experimental scatter. Furthermore, the substantial differences in normalized load capacities between both investigated ages indicates that other effects might be more dominant than the investigated aggregate effect. This observation is discussed in more detail by Nincevic et al. [47].

Normalized results according to Eq. (4) are shown in Fig. 4, both for the 28 day (a) and 70 day (b) results. For that purpose concrete modulus and total fracture energy obtained only from "moist-in" specimens are used. In this case the relative difference among the concretes is higher, approximately 11% on average for both ages. This increased relative difference has to be interpreted in the light of the typically quite large experimental scatter in fracture tests. Similar to the normalization by compressive strength also the normalization according to Eq. (2) fails to capture the increasing conservatism with age. While for 28 days the model predictions are almost perfect on average (N_{exp}/N_{EGF}= 1.03) the difference exceeds more than 30% at 70 days.

In conclusion, both investigated models are able to predict the concrete cone capacity of cast-in headed studs from standard concrete properties (i.e. compressive strength or the product of modulus and fracture energy) regardless of the coarse aggregate used, albeit the CCD method suggested more conservative capacities. The remaining error, independent of the concrete age and curing protocol, is in all cases within the expected experimental scatter. Consequently, from a practical point of view no aggregate effect exists. It can be expected that the standard concrete properties represent sufficiently well the material response for the purpose of determining the concrete cone capacity in tension. As discussed before, an objective quantitative measure, formulated analogous to the coefficient of variation, is considered rather than the mean value after normalization close to one. In this light, indeed the equation based on fracture energy yields predictions closer to one while the strength based equation reduces the scatter between concretes. The latter seems more relevant as we know that the particular k value is anchor geometry dependent.

These results confirm indications found by Rodriguez et al. [36] during a study on the behavior of expansion anchors under dynamic load. Also, the present results are in very good agreement with a previous study [48,49], in which the influence of aggregates on a typical undercut anchor product was investigated. In total, the aggregate effect on the concrete cone capacity has been studied on six concretes (two ages each) for two types of mechanical anchors with the same conclusions. Both studies also show that other effects may be more pronounced such as the age effect revealed and further discussed in [47].

4.2. Influencing factors

In this section the main influence factors on the concrete cone capacity are investigated. More specifically, this section presents the analysis of (i) the dependence of the pull-out capacities on the concrete properties obtained from "moist-in" cured specimens, (ii) the latter's dependence on the aggregate properties, (iii) the direct dependence of the system response on the aggregate properties. It has to be noted here that only concrete properties obtained from "moist-in" cured specimens are discussed. The presented investigation is not a rigorous correlation

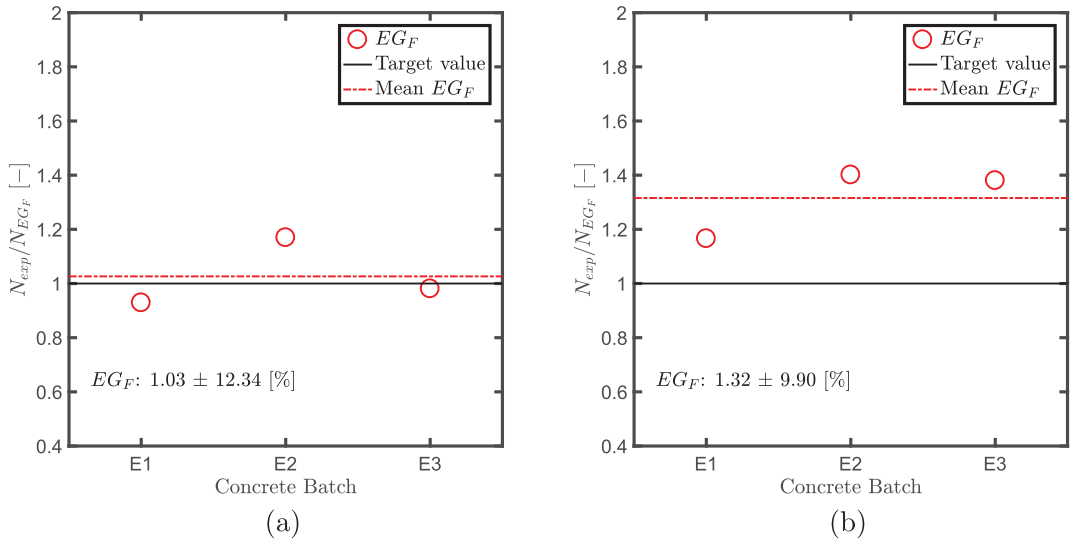

Fig. 4. Normalized concrete cone capacity using the fracture energy based prediction model according to Eq. (4) for (a) 28 days, and (b) 70 days results.

analysis but an attempt to visualize trends based on the limited data available which certainly is biased by the other arbitrarily varying material properties. However, considering all the testing and material parameters it is practically impossible to obtain experimental data in which only one parameter is varied. This could only be done in a statistical sense by compiling a large database of tests and forming sub populations for which the mean values of all properties except one are approximately constant, see e.g. [50]. The only other method would be suitable lower scale simulations in which indeed each parameters could be varied independently in virtual experiments.

A good measure of dependence between two random variables X and Y is Pearson's coefficient of linear correlation. The latter quantifies a relation of the variation of two variables and is defined by $\rho_{X,Y} = \mathrm{cov}(X, Y)/\sigma_X \sigma_Y$, where $\mathrm{cov}(X, Y)$ is their covariance, and σ_X and σ_Y are the sample standard deviations, which can be estimated by

$$\rho_{X,Y} = \frac{\sum_{i=1}^{n} X_i Y_i - n\overline{X}\,\overline{Y}}{\sqrt{\sum_{i=1}^{n} X_i^2 - n\overline{X}^2}\sqrt{\sum_{i=1}^{n} Y_i^2 - n\overline{Y}^2}} \tag{5}$$

with the measured values X_i, Y_i, the sample mean values $\overline{X}$ and $\overline{Y}$, and n= number of samples.

Since the aggregates are chemically inert, it can be assumed that their properties are constant in time. On the other hand, the material properties of concrete, and therefore of the anchor system, age. Consequently, a real aggregate effect should reveal itself as statistical dependence between system response and aggregate properties that is relatively independent of the testing age although the dependence may evolve as concrete matures. It has to be noted that the sample size is quite small, too small to derive any firm conclusions. Nevertheless, relevant insights and indications can be obtained.

4.2.1. Correlation between aggregate and concrete properties

First, a study of the correlation between the aggregate properties and the concrete properties is presented. In Fig. 5(a) the L.A. coefficient of the different aggregate types is plotted against the concrete cube compressive strength. The two magnitudes are negatively correlated, as expected, since larger L.A. coefficients indicate a "weaker" aggregate material that is more prone to abrasion. This can be noticed also in Fig. 5(b), where the measured aggregate hardness is plotted against the compressive strength.

Finally, the correlation between the aggregate modulus and the concrete properties (compressive and tensile strength, and total fracture energy) is estimated. Fig. 6(a) shows that the cube compressive strength and aggregate modulus are strongly correlated as well, independently of the concrete age. Furthermore, it is interesting to note that the sensitivity of the concrete properties to aggregate properties seem to be time-invariant for the concrete compressive strength, see parallel lines in Figs. 5 and 6(a). The concrete and aggregate moduli are fully correlated at 28 days, Fig. 6(b), while a weaker correlation is observed for the later age. However, the slope of the regression line increases indicating a stronger influence of the aggregate property at later ages. Interestingly, concrete E2 (limestone aggregate) shows a quite high mean modulus at 70 days, Fig. 6(b). Furthermore, for E2 the tensile strength (Fig. 6(c)) is substantially higher at both ages while the total fracture energy (Fig. 6(d)) is quite low compared to the other two concretes.

4.2.2. Correlation between concrete properties and concrete cone capacity

Naturally, the concrete cone capacity depends on the concrete properties. However, the question remains whether compressive strength (or the product of modulus and fracture energy) carries enough information to predict the concrete cone break out capacity or if other material properties better reflect the system behavior.

Fig. 7 presents the experimentally obtained concrete cone capacities for both ages depending on (a) the concrete cube compressive strength $f_{c,cu}$ and (b) the cylinder splitting strength $f_{t,spl}$. As expected, the compressive strength and the indirect tensile strength are highly correlated with the pull-out capacity. This supports the use of the compressive strength based prediction model according to Eq. (1). In this study also the best fitting exponent of the power-law is investigated. The best fit yields an exponent of $\simeq 1.5$ if data of both ages are used jointly. This is quite different from the proposed exponent of 0.5 in Eq. (1). This difference in fitted exponent can be explained by the different curing states at both ages since the compressive strength is just a proxy for those material properties that control the peak load in a fracture problem, i.e. tensile strength together with Young's modulus and fracture energy. This becomes clearer when the data of the individual ages are fitted separately. In that case exponents of 0.83 and 0.84 are obtained for 28 and 70 days, respectively, if the "dry-cured" cube compressive strength is used (Fig. 8).

Finally, the correlation between the concrete cone capacity and the modulus E, and the total fracture energy G_F is estimated. Fig. 9(a) shows that the modulus tested on moist cured cylinders is strongly correlated to the tested pull-out capacity. However, contrary to expectations the total fracture energy and the pull-out capacity show only a weak (and negative) correlation. This findings are in contradiction with the previously reported numerical study by Ožbolt [51] which showed that for a given concrete fracture energy, the concrete cone

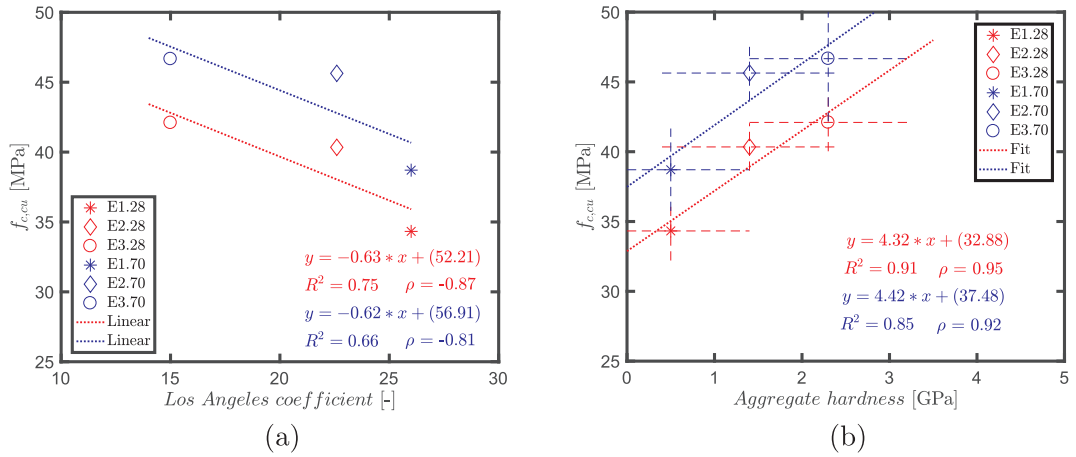

Fig. 5. Correlation between concrete "moist-in" cube compressive strength and (a) aggregate LA coefficient, (b) aggregate hardness.

failure load increases only slightly with the concrete tensile strength while for a given concrete tensile strength, the concrete cone failure load increases significantly with the concrete fracture energy G_f. The rate of increase was reported to be proportional to $G_f^{0.5}$. This trend cannot be seen in the presented analysis as all the material properties change, distorting the actual dependencies.

4.2.3. Correlation between aggregate properties and tensile capacity

The previous two subsections clearly revealed strong correlations between (i) aggregate hardness (or modulus) and concrete compressive strength, and (ii) concrete compressive strength (modulus) and concrete cone capacity. This subsection presents the main findings concerning the direct correlation between aggregate properties and experimentally obtained concrete cone capacities. Fig. 10 presents two examples of pairwise correlation plots that are representative for a large number of analyses performed. The pull-out capacities are only slightly correlated with the Los Angeles coefficient, revealing again that this parameter is not suitable for the characterization of the aggregate influence on the pull-out capacity. Fig. 10(b) shows a strong dependence of N_{exp} on the aggregate modulus. Almost identical results are obtained for aggregate hardness but omitted here. However, it is important to note that the regression lines for 28 and 70 days are far from parallel

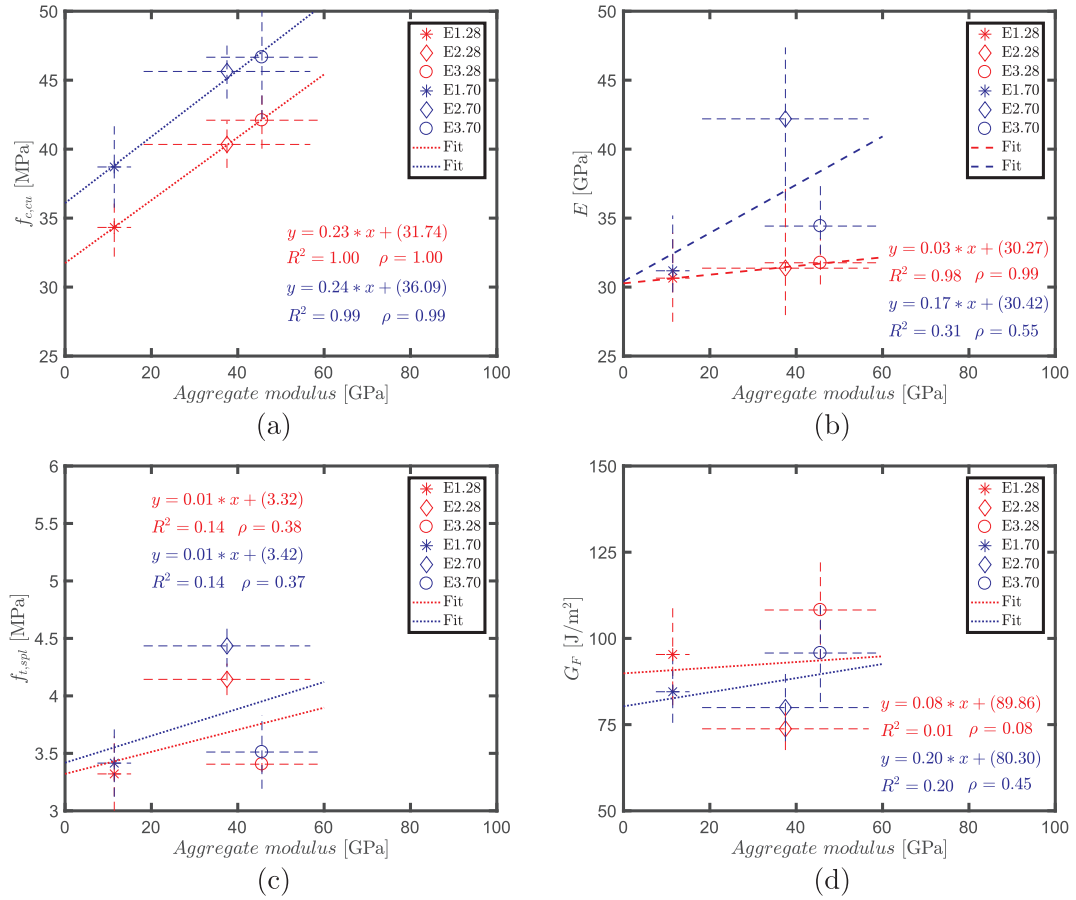

Fig. 6. Correlation between aggregate modulus and concrete "moist-in": (a) cube compressive strength, (b) modulus, (c) indirect tensile strength, and (d) total fracture energy.

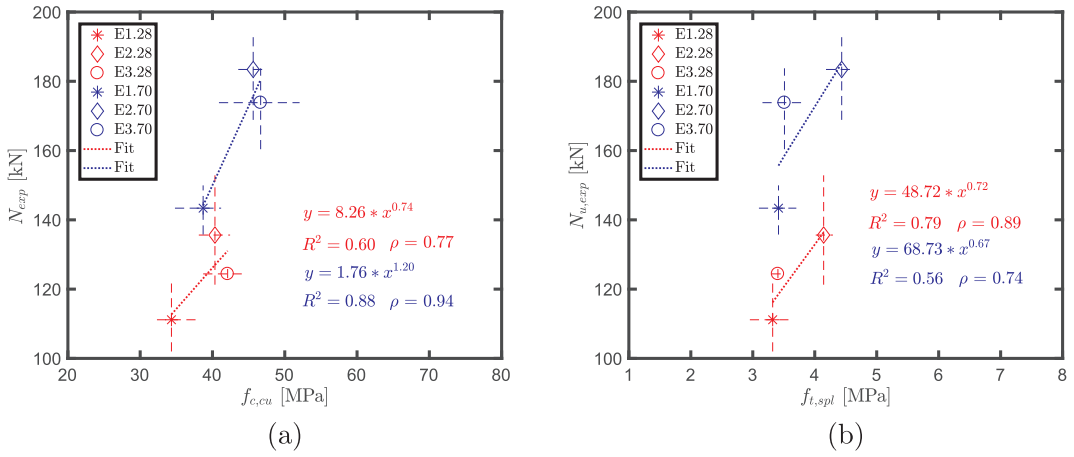

Fig. 7. Correlation between concrete cone capacity and concrete "moist-in" (a) cube compressive strength, and (b) indirect tensile strength.

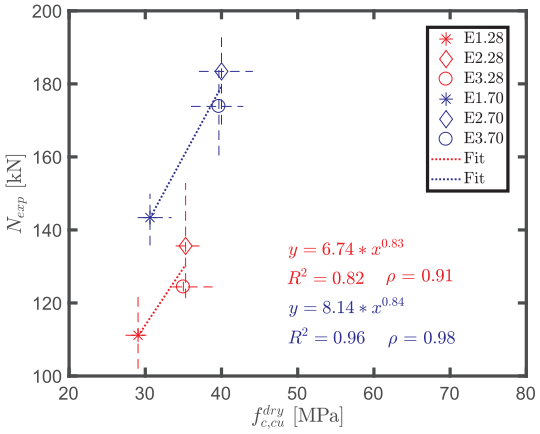

Fig. 8. Correlation between concrete cone capacity and concrete "dry" cube compressive strength.

(the slope almost doubles). This indicates a growing dependence on the mechanical aggregate properties as concrete matures and the performance of the cement paste increases. This growing dependence may explain the aging effect discussed earlier in this paper in Section 4.1 and Fig. 3 as well as in [47]. A further reason may be found in the fact that, macroscopically speaking, different material properties age at different rates [52,53].

It has to be noted that for the correlation analysis between aggregate properties and pull-out load capacity in Fig. 10 a linear trendline is used. The reason is that no specific functional dependence is expected and, thus, the simplest model is chosen due to the scarcity of data points. On the other hand, the power law relationship between concrete properties and the pull-out load capacities is well-established and has been adopted for this reason in some of the other analyses.

4.2.4. *Summary of correlation study*

Finally, the entire analysis based on the correlation between different components (aggregate, concrete, concrete cone capacity) can be summarized, as shown in Fig. 11. This schematic representation clearly reveals the dependence structure of all three components. The arrow width is scaled proportionally to the correlation value between 0 and 1.

Most available research either focuses on the influence of the coarse aggregate properties on the concrete properties or the dependence between concrete properties and system response (e.g. here pull-out capacity), although the latter relationship is often limited to compressive strength tests. In this contribution, both paths (solid line arrows) are covered systematically and concurrently for the same concretes. Additionally, also the direct link (dashed line arrows) between aggregate properties and system response (concrete cone capacity) is investigated. Based on the limited data set available it can be concluded that the concrete properties strongly depend on the aggregate properties and, in turn, highly influence the concrete capacity. It is interesting to note that the latter dependence is stronger than the direct correlation between concrete cone capacity and aggregate properties. Together with the normalization results presented earlier it can be concluded that both investigated models (Eq. (1) in terms of f_c and Eq. (2) in terms of EG_F) can be expected to predict accurately the concrete cone capacity

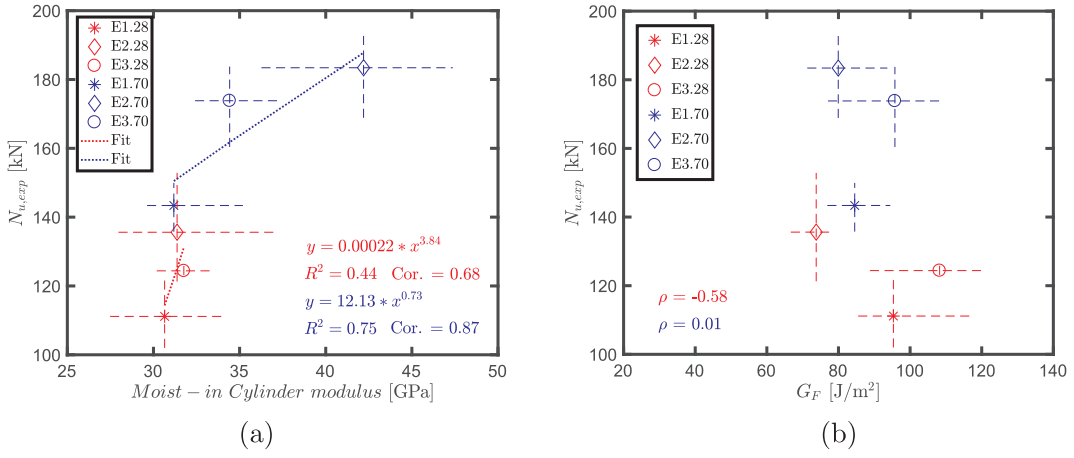

Fig. 9. Correlation between concrete cone capacity and concrete "moist-in" (a) modulus, and (b) total fracture energy.

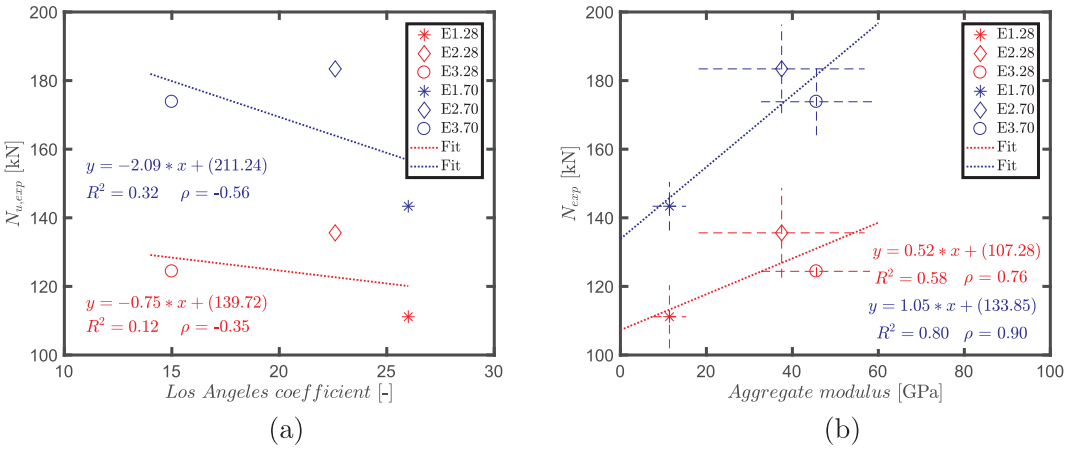

Fig. 10. Correlation between concrete cone capacity and (a) aggregate LA coefficient, (b) aggregate modulus.

irrespective of the used coarse aggregate type.

4.3. Cone shape analysis using photogrammetry

In reports and papers concrete cone sizes are generally expressed in terms of embedment depth and major/minor axes lengths assuming an ellipsoidal cone. A more precise way to document this geometrical information is photogrammetric analysis of the void left in the concrete slab after the break-out body is removed. The result of this measurement is a 3D point cloud that accurately describes the shape of the cone. To achieve that, several pictures of the crater left from the test need to be taken from different distances and angles. The next paragraph will describe the cone shape measurement for the current data.

The shape and curvature of the concrete cone is intrinsically linked to the failure mechanisms and the material properties. As such, it may provide insights into the effect that different aggregates have on the concrete cone capacity. Different aggregate properties and shapes would change locally the concrete properties and offer more or less resistance to the crack propagation. Fig. 12 shows the profiles of the average concrete cone of each individual set of tests in which the radial distance from the anchor axis (horizontal axis) is plotted against the distance from the surface (vertical axis). More details on the photogrammetric analysis are reported in a previous contribution [49]. Once all the individual cones have been processed, results belonging to the same group (age and aggregate) have been averaged. The figure shows that all concrete cones converge at both ends either to the anchor head or to the supporting ring. In spite of this the supports have no influence on the concrete cone capacity since the radius of the steel ring is twice the embedment depth. This geometry exceeds the empirically derived requirement for the inner diameter to be larger than $3h_{ef}$. The reason is

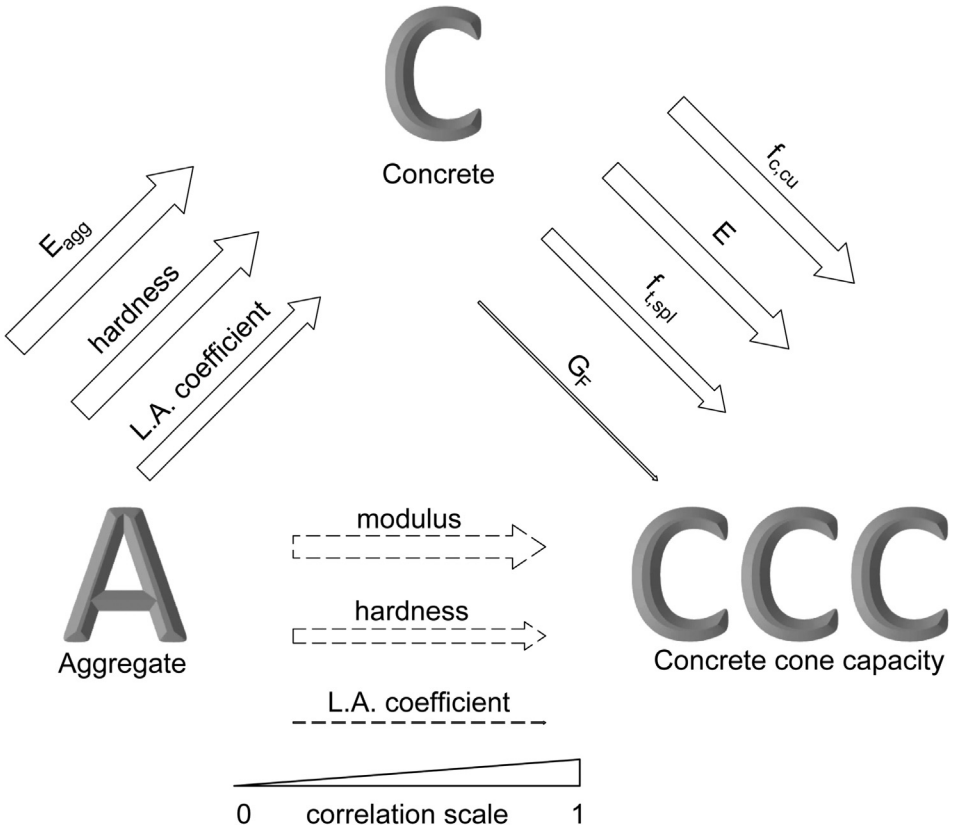

Fig. 11. Schematic representation of correlation between aggregate, concrete, and concrete cone capacity.

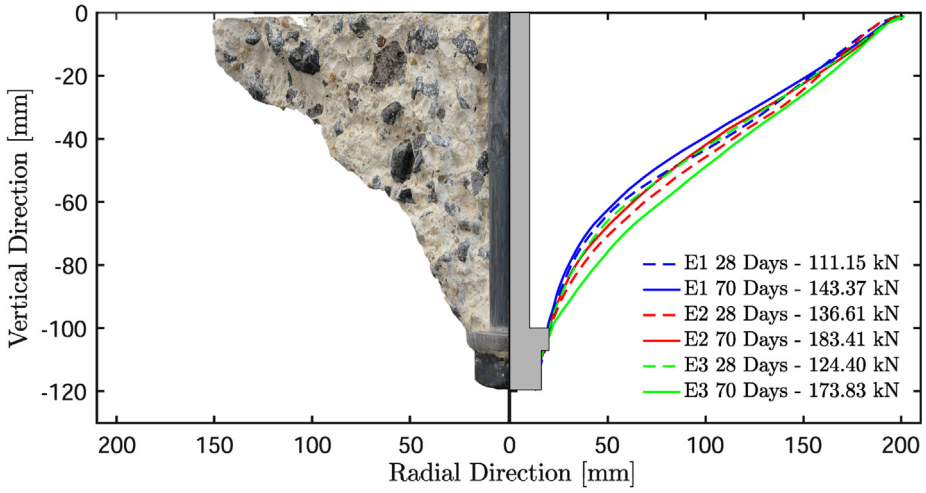

Fig. 12. Mean concrete cone profiles comparison.

that at peak load the crack only propagated about 40% of the total distance between anchor head and concrete surface [15]. From the results it can be seen that the difference among the batches is very small, compared to the maximum aggregate size. A visible trend though can be detected. E3 is associated with flatter concrete cone profiles, while E1 shows stronger curvature. Furthermore, for E1 and E2 stronger curvatures for later concrete ages can be noted.

5. Conclusions

After a brief state-of-the art review a comprehensive experimental campaign was presented comprising material characterization and pull-out tests on headed stud anchors for three normal strength concretes that differ almost exclusively in the petrography of the used coarse aggregate (basalt, limestone, and quartz) and size distribution. The experimentally obtained results are used (i) to evaluate the capabilities of the current predictive models with respect to the existence of an aggregate effect, and (ii) a sensitivity study on the influencing factors in an attempt to establish a link between aggregate properties, concrete properties, and concrete cone capacity. Finally, photogrammetrically obtained concrete cone shape profiles provide further insights into a link between coarse aggregate type and failure mechanisms.

Based on the presented systematic analysis that, however, still had to be limited to a specific headed stud anchor geometry and three concretes, the following conclusion can be drawn:

1. Differences in the petrography of the used aggregate and the aggregate size distribution result in different concrete properties (e.g. compressive and tensile strength), in spite of similar water to cement and aggregate to cement ratios. Concretes with limestone and basalt aggregate had similar compressive strengths, while the concrete with softer quartz aggregates resulted in a lower compressive strength (about 18%).
2. The concrete cone capacity is highly correlated to the concrete cube compressive strength. A correlation analysis shows that the concrete cone capacity is also strongly correlated to the concrete modulus, but only weakly to fracture energy. This is in contradiction with the results of previous research by Ožbolt [51] who showed numerically that the concrete cone capacity is strongly correlated with the concrete fracture energy.
3. Aggregate hardness and modulus are strongly correlated and, in turn, influence concrete properties. A strong correlation between aggregate modulus and concrete modulus as well as concrete compressive strength can be observed. The dependence of (indirect) tensile strength and fracture energy on aggregate properties is not as pronounced.
4. The experimentally obtained concrete cone capacities for the specific cast-in hex bolt of this investigation were checked against the currently established predictive equations in terms of compressive strength or the product of modulus and fracture energy. It is shown that the model in terms of compressive strength seems to conservatively underestimate the experimental values by around 20% at 28 days, and around 40% at 70 days, for all tested concretes. The fracture mechanics model formulated in terms of concrete modulus and fracture energy seems to be in a good agreement with the experiments at 28 days, and underestimates the experimental values by around 20% at 70 days.
5. Both currently established predictive models capture and account for the effect of different aggregates on the concrete cone capacity through the concrete properties. The remaining aggregate effect after normalization by the model predictions is less than 6%. This number can be considered insignificant (at least for practical purposes) compared to the typical experimental scatter in pull-out tests of 5% - 10%. Furthermore, the differences between ages exceed by far any remaining aggregate effect. The same conclusions have been obtained in a previous study on a post-installed undercut anchor [48,49]. In total, the aggregate effect has been studied on six concretes for two types of mechanical anchors (pre-installed and post-installed) and two ages each with the same conclusions.
6. A photogrammetric analysis performed on the concrete cones showed very small differences (small compared to the maximum aggregate size) among the different concretes. Therefore, it can be assumed that no significant aggregate effect on the concrete cone shape exists.

Acknowledgements

The financial support by the Austrian Federal Ministry for Digital and Economic Affairs and the National Foundation for Research, Technology and Development is gratefully acknowledged. Lisa-Marie Czernuschka is gratefully acknowledged for her contribution performing the concrete characterization tests, and Stefan Meißl for his support in performing the anchor pull-out tests and the data post-processing. Gabriel Pfuner is gratefully acknowledged for his support performing the photogrammetric analysis and detailed documentation during the experimental campaign.

Appendix A. Supplementary material

Supplementary data associated with this article can be found, in the

online version, at https://doi.org/10.1016/j.engstruct.2019.04.028.

References

[1] Mehta P, Monteiro P. Concrete: structure, properties, and materials; 2013.
[2] Kiliç A, Atiş CD, Ahmet Teymen, Karahan O, Özcan F, Bilim C, et al. The influence of aggregate type on the strength and abrasion resistance of high strength concrete. Cem Concr Compos 2008;30:290–6. https://doi.org/10.1016/j.cemconcomp.2007.05.011.
[3] Delmar LB, Gaynor RD. Effects of aggregate properties on strength of concrete. J Proc 1963;60:1429–56.
[4] Vilane BRT, Sabelo N. The effect of aggregate size on the compressive strength of concrete. J Agric Sci Eng 2016;2(6):66–9.
[5] Özturan Turan, Çeçen Cengizhan. Effect of coarse aggregate type on mechanical properties of concretes with different strengths. Cem Concr Res 1997;27(2):165–70. https://doi.org/10.1016/S0008-8846(97)00006-9. ISSN 0008-8846.
[6] Guinea G, El-Sayed K, Rocco C, Elices M, Planas J. The effect of the bond between the matrix and the aggregates on the cracking mechanism and fracture parameters of concrete. Cem Concr Res 2002;32:1961–70.
[7] CEN. Eurocode 2: Design of concrete structures – Part 1–1: General rules and rules for buildings, volume BS-EN-1992-1-1:2009. European Committee for Standardization; 2009.
[8] CEB-FIB. Model Code for Concrete Structures 2010. Ernst & Sohn; 2010.
[9] European Organisation for Technical Approvals (EOTA). Guideline for European Technical Approval of Metal Anchors For Use in Concrete. Part One: Anchors in General; European Organisation for Technical Approvals: Brussels, Belgium, volume ETAG 001; 1997.
[10] European Organisation for Technical Approvals (EOTA). Guideline for European Technical Approval of Metal Anchors For Use in Concrete. Part Two: Torque-Controlled Expansion Anchors; European Organisation for Technical Approvals: Brussels, Belgium, volume ETAG 001; 1997.
[11] European Organisation for Technical Approvals (EOTA). Guideline for European Technical Approval of Metal Anchors For Use in Concrete. Part Three: Undercut Anchors; European Organisation for Technical Approvals: Brussels, Belgium, volume ETAG 001; 1997.
[12] Guideline for European Technical Approval of Metal Anchors For Use in Concrete. Part Four: Deformation-Controlled Expansion Anchors; European Organisation for Technical Approvals: Brussels, Belgium, volume ETAG 001; 1998.
[13] Guideline for European Technical Approval of Metal Anchors For Use in Concrete. Part Five: Bonded Anchors; European Organisation for Technical Approvals: Brussels, Belgium, volume ETAG 001; 2002.
[14] Fuchs W, Eligehausen R, Breen JE. Concrete capacity design (CCD) approach for fastening to concrete. ACI Struct J 1995;92:73–94.
[15] Eligehausen R, Sawade G. A fracture mechanics based description of the pull-out behavior of headed studs embedded in concrete. Fract Mech Concr Struct 1989. https://doi.org/10.18419/opus-7930.
[16] Eligehausen R, Malle R, Silva J. Anchorage in concrete construction. Berlin: Ernst & Sohn; 2006.
[17] Ottosen NS. Nonlinear finite element analysis of pull-out test. J Struct Div ASCE 1981;107(4):591–603.
[18] Stone WC, Carino NJ. Deformation and failure in large-scale pullout tests. ACI J Proc 1983;80(6).
[19] Krenchel H, Shah SP. Fracture analysis of the pullout test. Mater Struct 1985;18(6):439–46.
[20] Ballarini R, Shah SP, Keer LM. Failure characteristics of short anchor bolts embedded in a brittle material. Proc Roy Soc Lond A: Math Phys Eng Sci 1986;404(1826):35–54.
[21] Eligehausen R, Sawade G, Verhalten von Beton auf Zug (Behavior of Concrete in Tension). Betonwerk und Fertigteil-Technik 5 und 6, 1985;51(5):315–22 [in German and English].
[22] Ozbolt J, Eligehausen R. Numerical analysis of headed studs embedded in large plain concrete blocks. In: Bicanic N, Mang H (Herausgeber), editors. Computer aided analysis and design of concrete structures. Lomdon: Pinerdige Press; 1990.
[23] ACI Committee. Code requirements for nuclear safety related concrete structures (ACI 349–85) (Revised 1990) (Reproved). ACI J 1985;82(8):349–85.
[24] Bazant ZP. Size effect in blunt fracture: concrete, rock, metal. J Eng Mech ASCE 1984;110:518–35.
[25] Bazant ZP, Planas J. Fracture and size effect in concrete and other quasibrittle materials. Boca Raton, Florida: CRC Press; 1998.
[26] Fornusek Jindrich, Konvalinka Petr. Numerical investigation of head diameter influence on tensile capacity of headed studs. In: ISBEIA 2012 – IEEE symposium on business, engineering and industrial applications; 2012. p. 737–41. https://doi.org/10.1109/ISBEIA.2012.6422988.
[27] Nilforoush R, Nilsson M, Elfgren L. Experimental evaluation of influence of member thickness, anchor-head size, and orthogonal surface reinforcement on the tensile capacity of headed anchors in uncracked concrete. J Struct Eng 2018;144:04018012.
[28] Nilforoush R, Nilsson M, Elfgren L, Ožbolt J, Hofmann J, Eligehausen R. Tensile capacity of anchor bolts in uncracked concrete: influence of member thickness and anchors head size. Struct J 2017;114:1519–30.
[29] ETAG 001: Metal Anchors for Use in Concrete – Annex A: Details of tests, European Organisation for technical Approvals (EOTA); 2012.
[30] Primavera EJ, Pinelli JP, Kalajian EH. Tensile behavior of cast-in-place and undercut anchors in high-strength concrete. Struct J 1997;94:583–94.
[31] Winters JB, Dolan CW. Concrete breakout capacity of cast-in-place concrete anchors in early-age concrete. PCI J 2014;59:114–31.
[32] Eligehausen R, Balogh T. Behavior of fasteners loaded in tension in cracked reinforced concrete. Struct J 1995;92:365–79.
[33] Obolt J, Eligehausen Rolf, Periškić G, Mayer U. 3D FE analysis of anchor bolts with large embedment depths. Eng Fract Mech 2007;74:168–78. https://doi.org/10.1016/j.engfracmech.2006.01.019.
[34] Ožbolt J, Kožar Ivica, Eligehausen Rolf, Periškić Goran. Three-dimensional FE analysis of headed stud anchors exposed to fire. Comput Concr 2005;2. https://doi.org/10.12989/cac.2005.2.4.249.
[35] Hordijk DA, van der pluijm R. Behaviour of fasteners in concrete with coarse recycled concrete and masonry aggregates. RILEM Publications SARL 2001:805–14.
[36] Rodriguez M, Lotze D, Gross JH, Zhang YG, Klingner RE, Graves HL. Dynamic behavior of tensile anchors to concrete. Struct J 2001;98:511–24.
[37] British Standard Institution (BSI). Testing hardened concrete. Making and curing specimens for strength tests. London, BS EN 12390-2 2009; 2009.
[38] ASTM. Standard practice for making and curing concrete test specimens in the laboratory. C192-14. West Conshohocken: ASTM International; 2014.
[39] Fischer-Cripps Anthony C. Nanoindentation. New York: Springer-Verlag New York, Inc.; 2002.
[40] Doerner MF, Nix WD. A method for interpreting the data from depth-sensing instruments. J Mater Res 1986;1:601–9.
[41] Oliver WC, Pharr GM. An improved technique for determining hardness and elastic modulus using load and displacement sensing indentation experiments. J Mater Res 1992;7:1564–83.
[42] British Standard Institutes, BS EN 1097-2:2010-03. Tests for mechanical and physical properties of aggregates, Part 2: Methods for the determination of resistance to fragmentation. British Standard Institution, London.
[43] British Standard Institutes, BS EN 12390-3:2009. Testing hardened concrete. Compressive strength of test specimens British Standard Institution, London.
[44] British Standard Institutes, BS EN 12390–6:2009. Testing hardened concrete. Tensile splitting strength of test specimens, British Standard Institution, London.
[45] Czernuschka L-M, Wan-Wendner R, Vorel J. Investigation of fracture based on sequentially linear analysis 202:75–86. https://doi.org/10.1016/j.engfracmech.2018.08.008.
[46] Hillerborg A. Analysis of one single crack; fracture mechanics of concrete (developments in civil engineering). Amsterdam, The Netherlands: Elsevier; 1983. p. 223–49.
[47] Ninčević K, Czernuschka LM, Marcon M, Wan-Wendner R. Age dependence of concrete cone capacity under tensile loading. ACI Struct Mater J 2018. [in press].
[48] Nincevic K, Czernuschka LM, Marcon M, Boumakis I, Wan-Wendner R. Aggregate effect in fastening applications; In: IABSE c/o ETH Hnggerber, Zrich, IABSE symposium, Vancouver, 2017, Engineering the Future, Report; 2017. ISBN: 978-3-85748-153-6.
[49] Marcon M, Ninčević K, Boumakis I, Czernuschka L-M, Wan-Wendner R. Aggregate effect on the concrete cone capacity of an undercut anchor under quasi-static tensile load. Materials 2018;11(5):711. https://doi.org/10.3390/ma11050711.
[50] Yu Q, Le J-L, Hubler MH, Wan-Wendner R, Cusatis G, Bazant ZP. Comparison of main models for size effect on shear strength of reinforced and prestressed concrete beams. Struct Concr 2016;17. https://doi.org/10.1002/suco.201500126.
[51] Ožbolt J. Maßstabseffekt und Duktilität von Beton-und Stahlbetonkonstruktionen (Size effect and ductility of concrete and reinforced concrete structures) [Thesis submitted for the certificate of habilitation]. IWB, Universität Stuttgart; 1995. [in German].
[52] Wan L, Wendner R, Benliang L, Cusatis G. Analysis of the behavior of ultra high performance concrete at earlyage. Cem Concr Compos 2016;74:120–35.
[53] Wendner R, Nincevic K, Boumakis I, Wan L. Age-dependent lattice discrete particle model for quasi-static simulations. Key Eng Mater 2016;711:1090–7.